




Short Note

# *N*-(Isobutyl)-3,4-methylenedioxy Cinnamoyl Amide

Aboagye Kwarteng Dofuor <sup>1,2</sup>, Samuel Kwain <sup>3</sup>, Enoch Osei <sup>3</sup>, Gilbert Mawuli Tetevi <sup>3</sup>,  
Laud Kenneth Okine <sup>1,2</sup>, Mitsuko Ohashi <sup>4</sup>, Theresa Manful Gwira <sup>1,2,\*</sup> and  
Kwaku Kyeremeh <sup>3,\*</sup>

<sup>1</sup> West African Center for Cell Biology of Infectious Pathogens, University of Ghana,  
P.O. Box LG 54 Legon-Accra, Ghana

<sup>2</sup> Department of Biochemistry, Cell and Molecular Biology, University of Ghana,  
P.O. Box LG 54 Legon-Accra, Ghana

<sup>3</sup> Marine and Plant Research Laboratory of Ghana, Department of Chemistry, School of Physical and  
Mathematical Sciences, University of Ghana, P.O. Box LG 56 Legon-Accra, Ghana

<sup>4</sup> Department of Parasitology, Noguchi Memorial Institute for Medical Research, University of Ghana,  
P.O. Box LG 581 Legon-Accra, Ghana

\* Correspondence: tmanful@ug.edu.gh (T.M.G.); kkyeremeh@ug.edu.gh (K.K.);  
Tel.: +233-204-752-176 (T.M.G.); +233-504-829-778 (K.K.)

Received: 19 June 2019; Accepted: 3 July 2019; Published: 5 July 2019



**Abstract:** The plant *Zanthoxylum zanthoxyloides* (Lam.) Zepern. & Timler is one of the most important medicinal species of the genus *Zanthoxylum* on the African continent. It is used in the treatment and management of parasitic diseases in sub-Saharan Africa. These properties have inspired scientists to investigate species within the genus for bioactive compounds. However, a study, which details a spectroscopic, spectrometric and bioactivity guided extraction and isolation of antiparasitic compounds from the genus *Zanthoxylum* is currently non-existent. Tortozanthoxylamide (**1**), which is a derivative of the known compound armatamide was isolated from *Z. zanthoxyloides* and the full structure determined using UV, IR, 1D/2D-NMR and high-resolution liquid chromatography tandem mass spectrometry (HRESI-LC-MS) data. When tested against *Trypanosoma brucei* subsp. *brucei*, the parasite responsible for animal African trypanosomiasis in sub-Saharan Africa, **1** (IC<sub>50</sub> 7.78 μM) was just four times less active than the commercially available drug diminazene aceturate (IC<sub>50</sub> 1.88 μM). Diminazene aceturate is a potent drug for the treatment of animal African trypanosomiasis. Tortozanthoxylamide (**1**) exhibits a significant antitrypanosomal activity through remarkable alteration of the cell cycle in *T. brucei* subsp. *brucei*, but it is selectively non-toxic to mouse macrophages RAW 264.7 cell lines. This suggests that **1** may be considered as a scaffold for the further development of natural antitrypanosomal compounds.

**Keywords:** trypanosomiasis; antitrypanosomals; cell cycle; cell viability; *Zanthoxylum*; *Rutaceae*; 1,3-benzodioxole; spectroscopy

## 1. Introduction

African trypanosomiasis (AT) is a tsetse-transmitted disease of humans and other animals caused by the parasitic protozoan that belongs to the *Trypanosoma* genus. Human African trypanosomiasis (HAT) afflicts an estimated 70 million people living in over 36 countries in sub-Saharan Africa [1] while animal African trypanosomiasis (AAT) continues to threaten the lives of several million herds of cattle every year [2]. Trypanosome infections cause considerable losses in health, economy and productivity of both humans and livestock every year. The prospects of vaccine development for the disease are beset with various challenges partly due to the several immune evasive strategies possessed by the rather resilient trypanosome parasite [3]. Chemotherapy is therefore the most efficient and

economically worthwhile option for treatment [4], but due to challenges caused by drug resistance, difficult and painful treatment routines, adverse side effects and several physicochemical challenges of existing drugs, there is currently an urgent need to discover new drugs for trypanosomiasis [5–9]. In order to meet this urgent need for a more efficient chemotherapy for trypanosomiasis, insights into possible target metabolic pathways for the action of antitrypanosomals are required alongside efficient and systematic screening (aided by spectroscopy, spectrometry and bioassays) of both plants and microbial natural products for novel leads.

In the last four years, our laboratory has been involved in a systematic screening of plants that are routinely used in several traditional remedies for the treatment and management of both HAT and AAT in several communities in Ghana, West Africa. The overall aim is to fully characterize the active principles behind the efficacy of these remedies. One of these plants belongs to the genus *Zanthoxylum* and is widely distributed in most temperate and subtropical zones of Africa, Asia, North America, South America and Australia [10]. The plant *Zanthoxylum zanthoxyloides* (Lam.) Zepern. & Timler is one of the most important medicinal species of the genus *Zanthoxylum* on the African continent.

The shrubs and trees of *Z. zanthoxyloides* are spiny and somewhat scandent in nature, ranging between 6 and 12 m in height [11,12]. The bark is of a grey to beige color with fine vertical fissures and woody prickle-bearing protuberances. The species also possesses a yellow odorous slash with characteristic solitary prickles on its stem. Its inflorescence consists of a lax terminal or axillary panicle with white or greenish flowers that could be regular or unisexual in nature [11,12]. *Z. zanthoxyloides* is known to possess pharmacologically useful phytochemicals such as acridones (hebelicine A), citronellol and divanilloylquinic acids (burkinabins A–C) [13–15]. These phytochemicals may be partly responsible for the trypanostatic effects observed after treatment of mice with *Z. zanthoxyloides* [16,17]. However, the exact chemical structures and mechanisms of action for the antitrypanosomal compounds produced by the plant have not been investigated in much detail. In this project, *Z. zanthoxyloides* was collected from the Centre for Plant Medicine Research (CPMR) in Mampong-Akuapem, Ghana. About 1 kg of the whole plant was extracted with cold percolation using dichloromethane followed by methanol. The dichloromethane and methanol extracts were combined and dried under vacuum to give a total crude extract (TCE). This crude extract was subjected to solvent partitioning using a modification of the Kupchan process [18] (Figure S16). A bioactivity, spectroscopy and spectrometry guided isolation process involving the use of thin layer and Sephadex LH20 chromatography followed by HPLC led to the discovery of a new derivative of armatamide [19]. The structure of this new compound was determined using a combination of IR, UV, 1D and 2D-NMR spectroscopy and high-resolution liquid chromatography tandem mass spectrometry (HRESI-LC-MS) techniques as *N*-(isobutyl)-3,4-methylenedioxy cinnamoyl amide (**1**). This new compound was found to exhibit selectively significant antitrypanosomal activity against *Trypanosoma brucei* subsp. *brucei* through a marked inhibition of the cell cycle phases of the parasite.

## 2. Results

Compound **1** (*N*-(isobutyl)-3,4-methylenedioxy cinnamoyl amide or tortozanthoxylamide) was obtained at  $t_R$  of 21 min on reverse phase HPLC. Compound **1** is a deep yellow oil when completely free of solvent. The HRESI-LC-MS of compound **1** gave  $m/z$  248.1281 for  $[M + H]^+$  corresponding to a molecular formula of  $C_{14}H_{18}NO_3^+$  with  $\Delta = \pm 0.6$  ppm and 7 degrees of unsaturation. An  $[M + Na]^+$  ion was also seen at  $m/z$  270.1095 belonging to the molecular formula  $C_{14}H_{17}NNaO_3^+$  ( $\Delta = +0.06$  and 7 degrees of unsaturation) which further and undoubtedly confirmed the mass of this new compound under electrospray ionization conditions. Compound **1** showed only one predominant fragment at  $m/z$  175.0428 corresponding to the formation of the acylium ion after cleavage of 2-methylpropan-1-amine from the parent structure (Figures S4–S6). This compound is an *N*-(isobutyl)-3,4-methylenedioxy cinnamoyl amide or tortozanthoxylamide (**1**). Analysis of the  $^1H$ ,  $^{13}C$  and multiplicity edited pulsed field gradient heteronuclear single quantum coherence (gHSQCAD) spectrum of **1**, suggested the presence of 14 carbons comprising four quaternary carbons, six methines, two methylenes and two

methyls. The  $^1\text{H-NMR}$  chemical shifts  $\delta_{\text{H}}$  6.94 (1H, d,  $J = 1.6$  Hz, H-2), 6.71 (1H, d,  $J = 8.0$  Hz, H-5) and 6.90 (1H, dd,  $J = 1.7, 8.1$  Hz, H-6) together with the  $\delta_{\text{C}}$  129.4 (C-1), 106.4 (C-2), 148.9 (C-3), 148.1 (C-4), 108.4 (C-5) and 123.7 (C-6) suggested a tri-substituted benzene ring with the substituents on C-3 and C-4 involving the same kind of heteroatom, oxygen. The coupling constants of  $\delta_{\text{H}}$  6.90 (1H, dd,  $J = 1.7, 8.1$  Hz, H-6) was direct indication that one of the three protons was isolated by the three substitutions on the benzene ring. Normally, substituted methylenes rarely appear at chemical shifts that are at higher ppm values than 70 ppm. Therefore, the  $\delta_{\text{H}}$  5.92 (2 H, s, H-14) with  $\delta_{\text{C}}$  101.4 (C-14) could only be accounted for by suggesting the presence of a 1,3-benzodioxole functionality in the chemical structure of **1**. These structure assignments were further confirmed by detailed analysis of the  $^1\text{H-}^1\text{H}$  homonuclear correlation spectroscopy (gCOSY) spectrum which showed the correlation H-5/H-6. Due to the presence of many quaternary atoms in this region, several pulsed field gradient  $^1\text{H-}^{13}\text{C}$  heteronuclear multiple bond correlations (gHMBCAD) were collected in order to further confirm the structure of this subunit. These correlations include, C-3, C-7, C-6 to H-2, C-4, C-1 to H-5 and C-3, C-7, C-2 to H-6. The  $\delta_{\text{H}}$  7.49 (1H, d,  $J = 15.5$  Hz, H-7), 6.33 (1H, d,  $J = 15.6$  Hz, H-8) and  $\delta_{\text{C}}$  140.4 (C-7), 119.2 (C-8) along with gHMBCAD correlations C-1 to H-8, C-1, C-2, C-6 to H-7 led to the conclusion that the tri-substituted 1,3-benzodioxole functionality was conjugated to a trans substituted double bond. The chemical shift step down  $\delta_{\text{C}}$  140.4 (C-7) to 119.2 (C-8) is characteristic for such systems and showed that the 1,3-benzodioxole functionality is on C-7 while C-8 is connected to a carbonyl. The gCOSY correlation H-7/H-8 along with gHMBCAD C-9, C-1, C-6, C-8, C-2 to H-7 and C-9, C-7, C-1 to H-8 provided evidence for the updated substructure. The carbon chemical shift  $\delta_{\text{C}}$  166.4 (C-9) was quite low compared to other carbonyls like those of ketones, aldehydes, esters and carboxylic acids and therefore assigned to an amide. Finally, the  $\delta_{\text{H}}$  0.91 (6H, d,  $J = 6.7$  Hz, H-13), 1.82 (1H, n,  $J = 6.7$  Hz, H-12), 3.17 (2H, t,  $J = 6.7$  Hz, H-11) and  $\delta_{\text{C}}$  47.2 (C-11) suggested the presence of a 2-methylpropan-1-amine moiety in the structure of **1**. All the gCOSY correlations H-5/H-6, H-7/H-8, H-13/H-12, H-12/H-11, H-13 and H-11/10NH, H-12 were further confirmed by similar  $^1\text{H-}^1\text{H}$  total correlation spectroscopy (2D-TOCSY) correlations, including H-5/H-6, H-7/H-8, H-11/10NH, H-12, H-13, H-12/10NH, H-11, H-13 and H-13/10NH, H-11, H-12. Analysis of the  $^1\text{H-}^1\text{H}$  rotating-frame Overhauser spectroscopy (ROESY) data gave only few correlations including H-7/H-8, H-11/H-12, H-12/H-11, H-13 and H-13/H-12. The complete NMR data for compound **1** are given in Table 1 while the raw data can be found in the Supplementary Figures S9–S15. In Figures 1 and 2, a visual representation of COSY, HMBC, 2D-TOCSY and ROESY correlations are shown. Furthermore, a new compound which is structurally unrelated to compound **1** due to the differences in fragmentation pattern was also detected in the crude solvent partitioning fraction of the plant at  $m/z$  224.2001 alongside the previously characterized compound armatamide (Figures S1, S7 and S8). The quantities of armatamide present were too low to facilitate purification. We may have missed the new eluting compound at  $m/z$  224.2001 during one of the chromatographic runs due to the fact that this metabolite did not have a strong UV absorbing chromophore and probably lacks activity. This represents a weakness in the techniques that we used because we are very likely to miss novel structures by virtue of their lack of UV chromophores in photodiode array PDA detection. However, using the HRESI-LC-MS data we were able to hypothesize that this compound was an analogue of the known structures lanyuamide I–III [20]. This hypothesis was based on the fact that in their mass spectrometry fragmentation pathways, lanyuamide I–III characteristically lose  $m/z = 58.0783$  corresponding to molecular formula  $\text{C}_4\text{H}_{10}$  which is an isobutyl functionality. Tortozanthoxylamide (**1**) also loses this fragment in its mass fragmentation pathway and since it is coming from the same genus, we proposed that it is similar in structure to lanyuamide I–III.

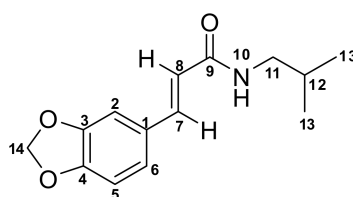


**Figure 1.** Structure of *N*-(isobutyl)-3,4-methylenedioxy cinnamoyl amide (**1**).

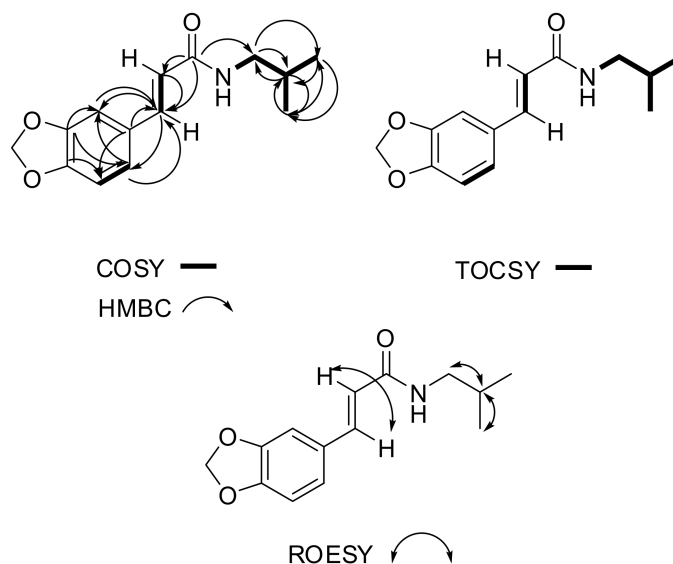


**Figure 2.** Key homonuclear correlation spectroscopy (COSY) and total correlation spectroscopy (TOCSY) (bold lines),  $^1\text{H}$ - $^{13}\text{C}$  HMBC (single arrows), rotating-frame Overhauser spectroscopy (ROESY) (double arrows) correlations for compound **1**.

**Table 1.** 1D and 2D-NMR spectroscopic data for compound **1** in  $\text{CDCl}_3$ , in ppm.

Signal Number	$\delta_{\text{C}}$ mult	$\delta_{\text{H}}$ mult (J Hz)	$^1\text{H}$ - $^1\text{H}$ COSY	$^1\text{H}$ - $^1\text{H}$ TOCSY	ROESY	HMBC
1	129.4, C					
2	106.4, CH	6.94, d (1.7)				C-3, C-7, C-6
3	148.9, C					
4	148.1, C					
5	108.4, CH	6.71, d (8.0)	6	6		C-4, C-1
6	123.7, CH	6.90, dd (1.7, 8.0)	5	5		C-3, C-7, C-2
7	140.4, CH	7.49, d (15.5)	8	8	8	C-9, C-1, C-6, C-8, C-2
8	119.2, CH	6.33, d (15.5)	7	7	7	C-9, C-7, C-1
9	166.4, C					
10NH		2.00				
11	47.2, $\text{CH}_2$	3.17, t (6.7)	10, 12	10, 12, 13	12	C-9, C-12
12	28.7, CH	1.82, n (6.7)	11, 13	10, 11, 13	11, 13	C-11, C-13,
13	20.2, $2\text{CH}_3$	0.91, d (6.7)	12	10, 11, 12	12	C-11, C-12, C-13
14	101.4, $\text{CH}_2$	5.92, s				

In order to determine its effects on the general metabolism of parasites, compound **1** was tested for its antitrypanosomal activity in a 48 h Alamar blue cell viability assay by employing the

absorbance property of resazurin (Figure 3). Normal cell lines (macrophages RAW 264.7) were also used to investigate its potential selectivity and toxicity profile. Compound 1 exhibited significant antitrypanosomal activity with an  $IC_{50}$  value of  $7.78 \mu\text{M}$  (Figure 3). It also displayed a relatively non-toxic selectivity profile with regards to its effects on mouse macrophages RAW 264.7,  $IC_{50} = 214.96 \mu\text{M}$  and selectivity index (SI) = 26.62 (Figure 3). Compound 1 was thus selective to *T. brucei* subsp. *brucei* as compared to mouse macrophages RAW 264.7 cell lines.

The cell cycle of trypanosomes involves four phases: G1, S, G2 and M phases [21]. Species from the genus *Zanthoxylum* have been reported previously to affect the cell cycle of different types of cells such as the human hepatoma-derived cell lines and human colon adenocarcinoma cell lines [22,23]. However, no compound isolated from the genus *Zanthoxylum* has been reported to inhibit the cell cycle of trypanosomes. The effect of compound 1 on the cell cycle phases of *T. brucei* subsp. *brucei* was thus investigated through flow cytometry (Figures 4 and 5; Table S1). There was a significant reduction of G0-G1 phase from 61.40% in the negative control to 55.0% in the presence of compound 1. Furthermore, there was a significant increase of S phase from 14.87% in the negative control to 18.80%. Compound 1 resulted in a significant increase of G2-M phase from 21.90% in the negative control to 25.83% (Figures 4 and 5; Table S1).

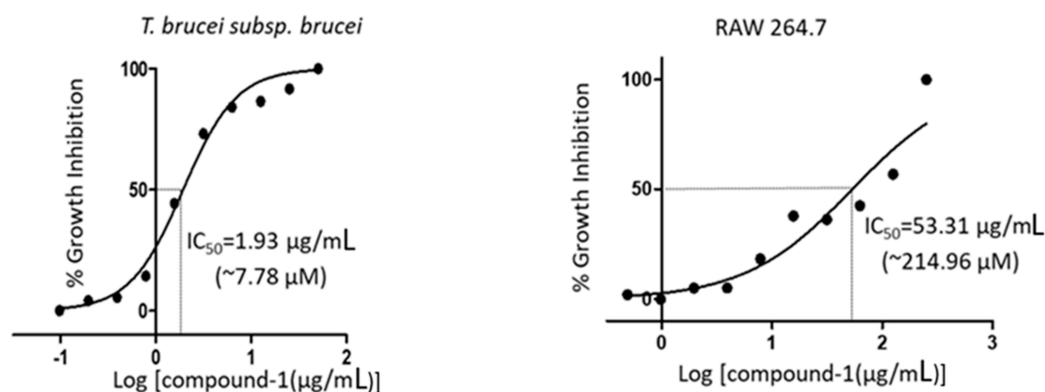


**Figure 3.** Dose-response curves for compound 1:  $IC_{50}$  values were calculated from Alamar blue cell viability assays in both *T. brucei* subsp. *brucei* and mouse macrophages RAW 264.7 cell lines. Selectivity index (SI = 27.62) was calculated as a ratio of the  $IC_{50}$  in *T. brucei* to that in RAW 264.7 cell lines.

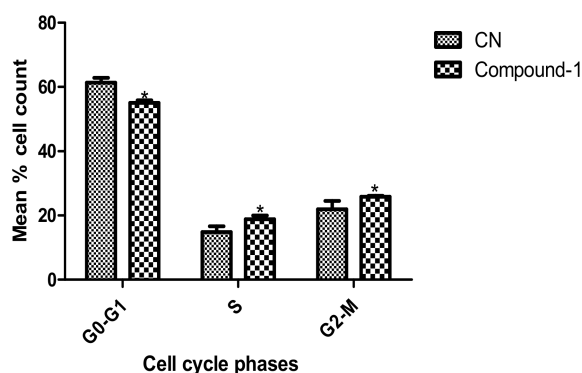


**Figure 4.** Effect of compound 1 on cell cycle of *T. brucei* subsp. *brucei*. The bar graph was plotted from the dot distributions in the cell cycle assay.  $P$ -values were calculated from four distinct counts [ $n = 4$ ;  $p \leq 0.05$  (\*, significant);  $p > 0.05$  (not significant)]. Error bars originate from mean percentage count  $\pm$  standard deviation of the mean (mean  $\pm$  SD). CN is Negative control.

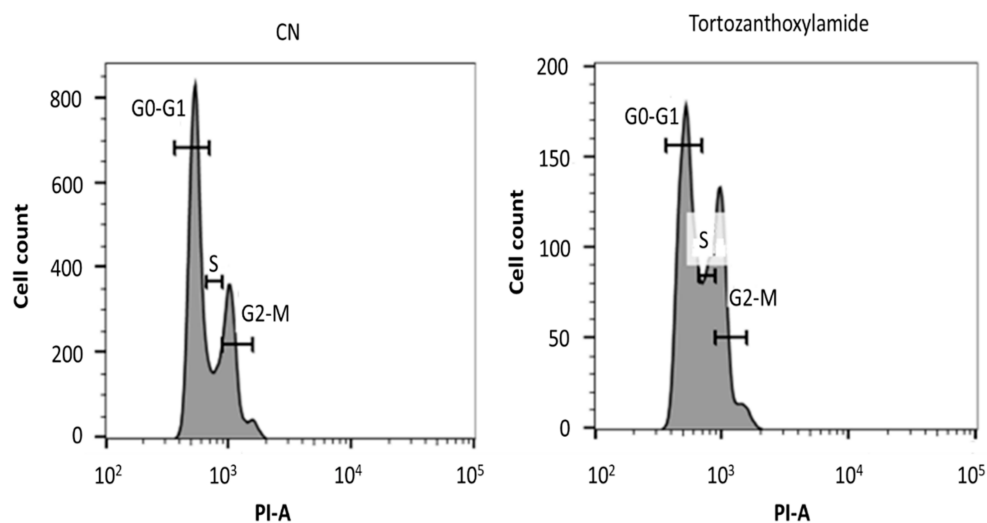


**Figure 5.** A typical histogram depicting the effects of tortozanthoxylamide (**1**) on the cell cycle phases (G0-G1, S and G2-M) of *T. brucei* subsp. *brucei*. PI is propidium iodide; CN is negative control.

The present study therefore, represents the first report of a compound isolated from the genus *Zanthoxylum* and shown to affect the cell cycle of trypanosomes. Since there was a significant reduction and increase in the G0-G1 and G2-M phases, respectively, compound **1** most probably constrained the parasites to the G2-M phase, thereby inhibiting karyokinesis and cytokinesis [21]. Compound **1** therefore, inhibited the complete separation of the parasites into two daughter cells after cell division, thereby potentially increasing the number of tetraploid cells at the G2-M phase. Moreover, compound **1** caused an increase in the S phase, which suggests possible inhibitory effects on DNA synthesis in *T. brucei* subsp. *brucei*.

### 3. Experimental Section

#### 3.1. General Experimental Procedures

1D and 2D NMR data were recorded on a Bruker AVANCE III HD Prodigy (BRUKER, Sylvenstein, Germany) at 500 and 125 MHz for  $^1\text{H}$  and  $^{13}\text{C}$ , respectively. This instrument was optimized for  $^1\text{H}$  observation with pulsing/decoupling of  $^{13}\text{C}$  and  $^{15}\text{N}$ , with 2H lock channels equipped with shielded z-gradients and cooled preamplifiers for  $^1\text{H}$  and  $^{13}\text{C}$ . The  $^1\text{H}$  and  $^{13}\text{C}$  chemical shifts were referenced to the solvent signals ( $\delta_{\text{H}}$  7.26 (1H, s) and  $\delta_{\text{C}}$  77.16 ppm in  $\text{CDCl}_3$ ). High-resolution mass spectrometry data were measured using a ThermoScientific LTQXL Linear Ion Trap High-resolution, Accurate-mass spectrometer-Discovery Orbitrap (Thermo Scientific, Bremen, Germany) coupled to an Accela Ultra Performance Liquid Chromatography-Diode Array Detection (UPLC-DAD) system. The following conditions were used for mass spectrometric analysis: capillary voltage 45 V, capillary temperature 320 °C, auxiliary gas flow rate 10–20 arbitrary units, sheath gas flow rate 40–50 arbitrary units, spray voltage 4.5 kV and mass range 100–2000 amu (maximum resolution 30,000). The ion source was normal electrospray ionization that acts both in positive and negative modes. Semi-preparative HPLC purifications were carried out using a Phenomenex Luna reverse-phase (C18 250 × 10 mm, L × i.d.) column connected to a Waters 1525 Binary HPLC pump Chromatograph with a 2998 photodiode array detector (PDA), column heater, and in-line degasser. Detection was achieved on-line through a scan of wavelengths from 200 to 400 nm. This system was also used to record the UV profile for the compound. IR was measured using a PerkinElmer Fourier Transform (FT)-IR (Universal Attenuated Total Reflection-UATR Two) spectrometer. All solvents were HPLC grade. Sephadex LH (Lipophilic-hydrophilic hydroxypropylated cross-linked dextran)-20 and HP (Polyaromatic adsorbent for hydrophobic compounds)-20 resin were obtained from Sigma Aldrich (Munich, Germany).

### 3.2. Plant Collection

The plant material, *Z. zanthoxyloides*, was collected from an arboretum of the Center for Plant Medicine Research (CPMR), Mampong-Akuapem, Ghana. It was authenticated by Herone Blagoege, a Senior Botanist at the Plant Development Department of CPMR. The plant material was given a voucher specimen number of CPMR 4120/4121/4122, air-dried and pulverized. The plant was collected at GPS coordinates 5°55'22.89'N and 0°06'20.75'W elev. 7 m; eye alt. 7.5 km.

### 3.3. Extraction and Purification

About 1 kg of the *Z. zanthoxyloides* whole plant was extracted under cold percolation conditions first with dichloromethane and followed by methanol. The sample was filtered after each extraction through a piece of glass wool under suction in a Buchner funnel to separate the filtrate from the plant debris. The methanol and dichloromethane extracts were combined and dried under vacuum with a Heidolph Rotavap at 40 °C and 1 atm pressure to give 1.5 g of total crude extract (TCE) of *Z. zanthoxyloides*. The TCE was suspended in 200 mL water and extracted three times with dichloromethane (600 mL). The remaining aqueous layer was then extracted once with sec-butanol and the butanol fraction was dried under vacuum to give the butanol/water (WB) fraction (0.5 g). The dichloromethane layer was dried under vacuum to give 0.9 g of extract which was suspended in a 9:1 mixture of methanol and water (200 mL). This fraction was then extracted three times with hexane (200 mL) after which the hexane layer was dried under vacuum to give a hexane fraction (FH) (0.2 g). The remaining 9:1 mixture of methanol and water layer was phase adjusted to a 1:1 mixture and extracted three times with dichloromethane which was dried under vacuum to give a dichloromethane fraction (FD) (0.6 g). The 1:1 methanol and water layer was also dried under vacuum to give a methanol/water (FM) fraction (0.1 g) (Figure S16). About 1 mg each of the four Kupchan solvent partitioning fractions (FH, FD, FM and WB) from *Z. zanthoxyloides* were submitted for high resolution electrospray ionization liquid chromatography tandem mass spectrometry (HRESI-LC-MS<sup>n</sup>). Analysis of the HRESI-LC-MS<sup>n</sup> data obtained for each solvent partitioning fraction in addition to testing antitrypanosomal biological activities and measurement of <sup>1</sup>H and <sup>13</sup>C-NMR suggested that the fraction of highest priority was FD (Table S2).

Semi-preparative normal phase thin layer chromatography (TLC) was repeatedly run for both Kupchan and gravity column fractions to estimate the levels of polarity and purity of all fractions, as well as to determine the appropriate solvent systems for subsequent chromatographic runs. The solvent systems used in TLCs were selected based on the Kupchan fractions (FH, FD, FM and WB) of interest. For the FD fractions, the solvents used were ethyl acetate, dichloromethane, *n*-hexane and occasionally methanol to facilitate the movement of highly polar compounds on normal phase. The data obtained from TLC runs were used to set up gravity column chromatography. Detection on TLC plates was facilitated by the use of UV lamps at both long (365 nm) and short (254 nm) wavelengths and phytochemical screening with the reagents iodine, ninhydrin, Dragendorff and antimony (III) chloride. For the ninhydrin and antimony (III) chloride tests, TLC spots were developed in 10% H<sub>2</sub>SO<sub>4</sub> with heating at 110 °C.

Silica gel gravity column chromatography was used in the further purification of Kupchan solvent partitioning fractions. The column used for this chromatographic step was 120 cm long and 2.5 cm wide with ethyl acetate, *n*-hexane and methanol routinely used as mobile phases. Briefly, the 600 mg FD fraction obtained from the *Z. zanthoxyloides* Kupchan solvent partitioning was loaded on a glass column containing silica gel packed to the 80 cm mark. The column was subjected to gradient elution using a mixture of *n*-hexane and ethyl acetate (90/10, 80/20, 70/30, 60/40, 50/50, 40/60, 30/70, 20/80 and 0/100). The remaining compounds on the silica column were then flushed out using 100% methanol. The column fractions obtained were dried under vacuum and labeled ZRFD-C1-C11 (17.7, 28.8, 83.8, 75.0, 21.1, 56.9, 29.3, 45.6, 17.7, 21.5 and 61.2 mg, respectively) in order of increasing polarities. The antitrypanosomal activities of the column fractions were determined (Table S2), after which fractions ZRFD-C3 (0.08 g) and ZRFD-C4 (0.08 g) were found to be the most

promising. Fraction ZRFD-C3 (0.08 g) was further purified by HPLC. HPLC separations were carried out using a Phenomenex Luna reverse-phase (C18 250 × 10 mm, L × i.d.) column connected to a Waters 1525 Binary HPLC pump Chromatograph with a 2998 PDA detector, column heater and in-line degasser. Detection was achieved on-line through a scan of wavelengths from 200 to 400 nm. Each injection took 60 min and started at time 0 min with solvent A (100% water) to 30 min with solvent B (100% acetonitrile) and hold at 100% acetonitrile for another 30 min. About 10.6 mg of the purified tortozanthoxylamide (**1**) was obtained after 48 h injections at  $t_R$  of 21 min and submitted for NMR data acquisition.

#### 3.4. *N-(Isobutyl)-3,4-Methylenedioxy Cinnamoyl Amide (1)*

Deep yellow pungent oil; IR (neat)  $\nu_{\max}$  3410, 3003, 2916, 1658, 1436, 1406, 1314, 1015, 951, 703  $\text{cm}^{-1}$ ; UV ( $\text{H}_2\text{O}:\text{CH}_3\text{CN}$ )  $\lambda_{\max}$  226, 278, 320 nm; for  $^1\text{H}$  and  $^{13}\text{C}$  NMR data, see Table 1; Mass spectrometry data is detailed in Supplementary Figure S4–S6.

#### 3.5. *Culture of Parasites and Mammalian Cell Lines*

Blood stream forms of *T. brucei* subsp. *brucei* (GUTat 3.1 strains) were cultivated in vitro to the logarithm phase using Hirim's Modified Iscove's Media (HMI9, Thermo Fisher Scientific) supplemented with 10% foetal bovine serum (Thermo Fisher Scientific) at 5%  $\text{CO}_2$  and 37 °C. Macrophages (RAW 264.7 cell lines) were cultivated in vitro to the logarithm phase using Dulbecco's Modified Eagle Media (DMEM, Thermo Fisher Scientific) with 10% foetal bovine serum at 5%  $\text{CO}_2$  and 37 °C.

#### 3.6. *Analysis of Cell Viability*

For *T. brucei* subsp. *brucei*, cells were seeded at a density of  $3.0 \times 10^5$  cells/mL in 96 well plates at two-fold dilution of fractions and incubated for 24 h. Alamar blue dye (10% V/V) was added to wells and incubated for another 24 h.

For mouse macrophages (RAW 264.7), cell lines were plated at a density of  $3.0 \times 10^5$  cells/mL for 48 h to allow for sufficient adherence to plates. Compounds were added to cells in a two-fold dilution and incubated for another 24 h. Alamar blue dye (10% V/V) was added to wells and incubated for another 24 h to allow for sufficient change in color of the dye. Experiments were run in quadruplicates. Spectrophotometric absorbances were recorded at a wavelength of 570 nm.

#### 3.7. *Analysis of Cell Cycle*

Cells were seeded at a density of  $3.0 \times 10^5$  cells/mL in 25  $\text{cm}^2$  culture dish with or without compounds for 24 h and centrifuged at 1700 rpm for 10 min. Cell pellets were suspended in 1.5 mL of 1× phosphate-buffered saline (PBS) and vortexed. Absolute ethanol was added (3.5 mL, final concentration of 70%) to fix cells at  $-20$  °C for 1 h. Cells were centrifuged at 1700 rpm for 10 min. Cell pellets were suspended with 200  $\mu\text{L}$  of guava cell cycle reagent that contains propidium iodide as a DNA-binding stain (EMD, Millipore). Suspended cells were added to wells containing the same volume of fresh guava cell cycle reagent. Cells were incubated for 30 min in darkness at room temperature. Distribution of cells at distinct cell cycle phases was measured with the BD LSFortessa X-20 flow cytometer.

#### 3.8. *Statistical Analysis*

Data from the cell viability assay was analyzed with Graphpad Prism version 5. The half-maximal inhibitory concentration ( $\text{IC}_{50}$ ) was calculated as the concentration that caused a 50% reduction in cell viability.  $\text{IC}_{50}$  values were calculated from a non-linear regression model as statistically appropriate. Histograms of cell cycle assays were analyzed with the BD FACSDiva 8.0.1 and FlowJo



V10. Graphpad Prism version 5 was employed for the analysis of unpaired *t*-test. *P*-values  $\leq 0.05$  were considered to be significant.

#### 4. Conclusions

The genus *Zanthoxylum* is a copious producer of many structurally intriguing and biologically active compounds [24]. This explains why several species belonging to the genus are found in many remedies used in the treatment and management of several diseases in sub-Saharan Africa and the rest of the world. Herein we have shown that a bioassay, spectroscopic and spectrometric guided extraction and isolation procedure for plants belonging to the genus could lead to the discovery of scaffolds that could form the starting points for the development of future antiparasitic agents. This technique can be extended to the discovery of novel scaffolds for other diseases such as infection and cancer. Tortozanthoxylamide (1) is produced by the Ghanaian *Z. zanthoxyloides* species collected and identified by the Center for Plant Medicine Research (CPMR), Mampong-Akuapem, Ghana. Generally, the 1,3-benzodioxole moiety in compound 1 can be found in the structures of many metabolites produced by plants such as *Astrodaucus persicus* (Boiss.) Drude [25]. Within the genus *Zanthoxylum*, several species such as *Zanthoxylum armatum* DC., *Zanthoxylum acanthopodium* DC. and *Zanthoxylum heitzii* (Aubrev. and Pellegr.) P.G. Waterman also produce compounds containing the 1,3-benzodioxole moiety [19,24,26]. The discovery of a new compound based on the 1,3-benzodioxole moiety in *Z. zanthoxyloides* is completely in line with the chemistry of such plants. Also, the fact that armatamide was detected in the extracts presupposes some similarities in the biosynthesis of these secondary metabolites.

Tortozanthoxylamide (1) exhibited significant antitrypanosomal activity with an  $IC_{50}$  value of 7.78  $\mu M$  compared to the commercially available drug diminazene aceturate ( $IC_{50}$  1.88  $\mu M$ ). It also displayed a relatively non-toxic selectivity profile with regard to its effects on mouse macrophages RAW 264.7,  $IC_{50} = 214.96 \mu M$  and selectivity index (SI) = 26.62. Hence, compound 1 has the potential to be bioactive against *T. brucei* subsp. *brucei* while at the same time producing little or no effects on normal cells. This result is interesting, given that the drug diminazene aceturate which is used to treat bacteria and protozoan infections in animals is significantly toxic [27–30].

**Supplementary Materials:** The supplementary materials are available online.

**Author Contributions:** M.O. conceptualized the research. A.K.D., T.M.G. and L.K.O. collected all the plants used in connection with this project. K.K., A.K.D., S.K., E.O. and G.M.T. performed the extraction and Kupchan solvent partitioning processes. A.K.D. and T.M.G. performed bioactivity studies of the Kupchan solvent partitioning fractions while K.K. performed NMR and MS studies of the fractions. K.K., T.M.G. and L.K.O. integrated the results of bioactivity, spectroscopy and spectrometry to prioritize FD as the fraction of interest. K.K., S.K., E.O. and G.M.T. conducted further purification and isolation processes with the support of bioactivity data provided by A.K.D. and T.M.G. K.K. measured all the IR, UV, NMR and MS data and solved the structure of the compound. Further bioactivity studies on the pure compound were performed solely by A.K.D., T.M.G. and L.K.O. K.K. and A.K.D. wrote the article.

**Funding:** This work was supported by funds from a World Bank African Centres of Excellence grant (ACE02-WACCBIP: Awandare) and a DELTAS Africa grant (DEL-15-007: Awandare). The DELTAS Africa Initiative is an independent funding scheme of the African Academy of Sciences (AAS)'s Alliance for Accelerating Excellence in Science in Africa (AESA) and supported by the New Partnership for Africa's Development Planning and Coordinating Agency (NEPAD Agency) with funding from the Wellcome Trust (107755/Z/15/Z: Awandare) and the UK government. The views expressed in this publication are those of the authors and not necessarily those of AAS, NEPAD Agency, Wellcome Trust or the UK government. KK wishes to thank the Centre for African Wetlands (CAW), University of Ghana, for providing seed funding and a TWAS Research Grant Award\_17-512 RG/CHE/AF/AC\_G. K.K. is also very grateful to the Cambridge-Africa Partnership for Research Excellence (CAPREx), which is funded by the Carnegie Corporation of New York, for a Postdoctoral Fellowship. K.K. also appreciates the Cambridge-Africa ALBORADA Research Fund for support and MRC African Research Leaders MR/S00520X/1 Award. S.K. wishes to thank the Carnegie BANGA-Africa Project Award for a PhD scholarship.

**Acknowledgments:** All the authors extend their gratitude to the Department of Chemistry, UG for providing NMR facility. We are also grateful to the West African Centre for Cell Biology of Infectious Pathogens, University of Ghana, for providing the BD LSFortessa X-20 flow cytometer.

**Conflicts of Interest:** The authors declare no conflict of interests.

## References

1. Simarro, P.P.; Cecchi, G.; Franco, J.R.; Paone, M.; Diarra, A.; Ruiz-Postigo, J.A.; Fèvre, E.M.; Mattioli, R.C.; Jannin, J.G. Estimating and Mapping the Population at Risk of Sleeping Sickness. *PLoS Negl. Trop. Dis.* **2012**, *6*, e1859. [[CrossRef](#)] [[PubMed](#)]
2. Morrison, L.J.; Vezza, L.; Rowan, T.; Hope, J.C. Animal African Trypanosomiasis: Time to Increase Focus on Clinically Relevant Parasite and Host Species. *Trends Parasitol.* **2016**, *32*, 599–607. [[CrossRef](#)] [[PubMed](#)]
3. Cnops, J.; Magez, S.; De Trez, C. Escape mechanisms of African trypanosomes: Why trypanosomosis is keeping us awake. *Parasitology* **2015**, *142*, 417–427. [[CrossRef](#)] [[PubMed](#)]
4. Steverding, D. The development of drugs for treatment of sleeping sickness: A historical review. *Parasites Vectors* **2010**, *3*, 15. [[CrossRef](#)] [[PubMed](#)]
5. Scott, A.G.; Tait, A.; Turner, C.M. Characterisation of cloned lines of *Trypanosoma brucei* expressing stable resistance to MelCy and suramin. *Acta Trop.* **1996**, *60*, 251–262. [[CrossRef](#)]
6. Matovu, E.; Geiser, F.; Schneider, V.; Maser, P.; Enyaru, J.C.; Kaminsky, R.; Gallati, S.; Seebeck, T. Genetic variants of the *TbAT1* adenosine transporter from African trypanosomes in relapse infections following melarsoprol therapy. *Mol. Biochem. Parasitol.* **2001**, *117*, 73–81. [[CrossRef](#)]
7. Baker, N.; Alsford, S.; Horn, D. Genome-wide RNAi screens in African trypanosomes identify the nifurtimox activator NTR and the eflornithine transporter AAT6. *Mol. Biochem. Parasitol.* **2011**, *176*, 55–57. [[CrossRef](#)]
8. Barrett, M.P.; Vincent, I.M.; Burchmore, R.J.; Kazibwe, A.J.; Matovu, E. Drug resistance in human African trypanosomiasis. *Fut. Microbiol.* **2011**, *6*, 1037–1047. [[CrossRef](#)]
9. Franco, J.R.; Simarro, P.P.; Diarra, A.; Ruiz-Postigo, J.A.; Samo, M.; Jannin, J.G. Monitoring the use of nifurtimox-eflornithine combination therapy (NECT) in the treatment of second stage gambiense human African trypanosomiasis. *Res. Rep. Trop. Med.* **2012**, *3*, 93–101. [[CrossRef](#)]
10. Patino, L.O.J.; Prieto, R.J.A.; Cuca, S.L.E. *Zanthoxylum* Genus as Potential Source of Bioactive Compounds. In *Bioactive Compounds in Phytomedicine*; Rasooli, I., Ed.; IntechOpen: Rijeka, Croatia, 2011; pp. 185–218.
11. Nacoulma, O. *Plantes Médicinales et Pratiques Médicales Traditionnelles au Burkina Faso Cas du Plateau Central*. Ph.D. Thesis, Université de Ouagadougou, Ouagadougou, Burkina Faso, 1996.
12. Arbonnier, M. *Trees, Shrubs and Lianas of West African Dry Zones*; CIRAD Margraf Publishers GMBH MNHN: Paris, France, 2004; p. 573.
13. Ngassoum, M.B.; Essia-ngang, J.J.; Tatsadjieu, L.N. Antimicrobial study of essential oils of *Ocimum gratissimum* leaves and *Zanthoxylum xanthoxyloides* fruits from Cameroon. *Fitoterapia* **2003**, *74*, 284–287. [[CrossRef](#)]
14. Ouattara, B.; Angenot, L.; Guissou, P.; Fondu, P.; Dubois, J.; Frédérick, M.; Jansen, O.; Van Heugen, J.C.; Wauters, J.N.; Tits, M. LC/MS/NMR analysis of isomeric divanilloylquinic acids from the root bark of *Fagara zanthoxyloides* Lam. *Phytochem.* **2004**, *65*, 1145–1151. [[CrossRef](#)] [[PubMed](#)]
15. Wouatsa, V.N.A.; Misra, L.; Kumar, S.; Prakash, O.; Khan, F.; Tchoumboungang, F.; Venkatesh, R.K. Aromatase and glycosyl transferase inhibiting acridone alkaloids from fruits of Cameroonian *Zanthoxylum* species. *Chem. Cent. J.* **2013**, *7*, 1–15. [[CrossRef](#)] [[PubMed](#)]
16. Mann, A.; Ifarajimi, O.R.; Adewoye, A.T.; Ukam, C.; Udeme, E.E.; Okorie, I.I.; Sakpe, M.S.; Ibrahim, D.R.; Yahaya, Y.A.; Kabir, A.Y.; et al. In vivo antitrypanosomal effects of some ethnomedicinal plants from Nupeland of north central Nigeria. *Afr. J. Tradit. Complement. Altern. Med.* **2011**, *8*, 15–21. [[CrossRef](#)] [[PubMed](#)]
17. Mann, A.; Ogbadoyi, E.O. Evaluation of Medicinal Plants from Nupeland for Their in vivo Antitrypanosomal Activity. *Am. J. Biochem. Mol. Biol.* **2012**, *2*, 1–6. [[CrossRef](#)]
18. Kupchan, S.M.; Britton, R.W.; Ziegler, M.F.; Sigel, C.W. Bruceantin, a new potent antileukemic simaroubolide from *Brucea antidysenterica*. *J. Org. Chem.* **1973**, *38*, 178–179. [[CrossRef](#)] [[PubMed](#)]
19. Kalia, N.K.; Singh, B.; Sood, R.P. A new amide from *Zanthoxylum armatum*. *J. Nat. Prod.* **1999**, *62*, 311–312. [[CrossRef](#)] [[PubMed](#)]
20. Chen, I.S.; Chen, T.L.; Lin, W.Y.; Tsai, I.L.; Chen, Y.C. Isobutylamides from the fruit of *Zanthoxylum integrifoliolum*. *Phytochemistry* **1999**, *52*, 357–360. [[CrossRef](#)]
21. Vaughan, S.; Gull, K. The structural mechanics of cell division in *Trypanosoma brucei*. *Biochem. Soc. Trans.* **2008**, *36*, 421–424. [[CrossRef](#)]

22. Chou, S.T.; Peng, H.Y.; Chang, C.T.; Yang, J.S.; Chung, H.K.; Yang, S.T.; Wood, W.G.; Chung, J.G. *Zanthoxylum ailanthoides* Sieb and Zucc. extract inhibits growth and induces cell death through G2/M-phase arrest and activation of apoptotic signals in colo 205 human colon adenocarcinoma cells. *Anticancer Res.* **2011**, *31*, 1667–1676.
23. Dung, T.D.; Chang, H.C.; Binh, T.V.; Lee, M.R.; Tsai, C.H.; Tsai, F.J.; Kuo, W.W.; Chen, L.M.; Huang, C.Y. *Zanthoxylum avicennae* extracts inhibit cell proliferation through protein phosphatase 2A activation in HA22T human hepatocellular carcinoma cells in vitro and in vivo. *Int. J. Mol. Med.* **2012**, *29*, 1045–1052.
24. Bhatt, V.; Kumar, N.; Sharma, U.; Singh, B. Comprehensive metabolic profiling of *Zanthoxylum armatum* and *Zanthoxylum acanthopodium* leaves, bark, flowers and fruits using ultra high performance liquid chromatography. *Sep. Sci. Plus* **2018**, *1*, 311–324. [[CrossRef](#)]
25. Goodarzi, S.; Hadjiakhoondi, A.; Yassa, N.; Khanavi, M.; Tofighi, Z. New benzodioxole compounds from the root extract of *Astrodaucus persicus*. *Iran. J. Pharm. Res.* **2016**, *15*, 901–906. [[PubMed](#)]
26. Goodman, C.D.; Austarheim, I.; Mollard, V.; Mikolo, B.; Malterud, K.E.; McFadden, G.I.; Wangenstein, H. Natural products from *Zanthoxylum heitzii* with potent activity against the malaria parasite. *Malar. J.* **2016**, *15*, 481. [[CrossRef](#)] [[PubMed](#)]
27. Wu, S.Y.; Park, G.Y.; Kim, S.H.; Hulme, J.; An, S.S.A. Diminazene aceturate: An antibacterial agent for shiga-toxin-producing *Escherichia coli* O157:H7. *Drug Des. Devel. Ther.* **2016**, *10*, 3363–3378. [[CrossRef](#)] [[PubMed](#)]
28. Kuriakose, S.; Muleme, H.; Onyilagha, C.; Okeke, E.; Uzonna, J.E. Diminazene aceturate (Berenil) modulates LPS induced pro-inflammatory cytokine production by inhibiting phosphorylation of MAPKs and STAT proteins. *Innate Immun.* **2014**, *20*, 760–773. [[CrossRef](#)]
29. Han, D.; Yoon, W.K.; Hyun, C. Cerebellar encephalopathy from diminazene aceturate (beneril) toxicity in a dog. *Korean J. Vet. Res.* **2014**, *54*, 193–196. [[CrossRef](#)]
30. Baldissera, M.D.; Bottari, N.B.; Rech, V.C.; Nishihira, V.S.; Oliveira, C.B.; Cargnin, L.P.; Moresco, R.N.; Thomé, G.R.; Schetinger, M.R.C.; Morsch, V.M.; et al. Combination of diminazene aceturate and resveratrol reduces the toxic effects of chemotherapy in treating *Trypanosoma evansi* infection. *Comp. Clin. Path.* **2016**, *25*, 137–144. [[CrossRef](#)]



© 2019 by the authors. Licensee MDPI, Basel, Switzerland. This article is an open access article distributed under the terms and conditions of the Creative Commons Attribution (CC BY) license (<http://creativecommons.org/licenses/by/4.0/>).